J|A|C|S
COMMUNICATIONS

Published on Web 12/02/2005

Engineering Pt in Ceria for a Maximum Metal−Support Interaction in Catalysis

Connie M. Y. Yeung,† Kai Man K. Yu,† Qi Jia Fu,† David Thompsett,‡ Michael I. Petch,‡ and Shik Chi Tsang*,†

Surface and Catalysis Research Centre, School of Chemistry, University of Reading, Whiteknights, Reading, RG6 6AD, U.K., and Johnson Matthey Technology Centre, Sonning Common, Reading RG4 9NH, U.K.

Received September 5, 2005; E-mail: s.c.e.tsang@reading.ac.uk

Traditional supported metal catalysts are comprised of small metal particles dispersed on the internal surface of an oxide support. Catalytic activity and selectivity of the catalyst are commonly found to be dependent on the type of metal and support used.[1] A great deal of research has been devoted to understanding this metal−support interaction in order to tailor the interaction for optimum catalysis. However, most conventional support and metal surfaces are structurally non-uniform; thus, the structures of supported metal catalysts are not well understood. Noble metal (NM)/ceria-based catalysts are among the systems long known to exhibit strong metal−support interaction (SMSI) effects.[2] These catalysts have been shown to give high activity for hydrogenation reactions, water−gas shift reactions, CO and hydrocarbon oxidation, etc.[2−9] It would be interesting to investigate encapsulated metal in ceria of controlled size as a more well-defined nanocatalyst, which would give the maximum degree of metal−support interaction in three dimensions (in contrast to two-dimensional model of NM on ceria). There have been some interesting works on the encapsulation of metal in metal oxide of different natures via co-precipitation reported in the literature.[7−9] However, conventional techniques like this cannot give the levels of control required to systematically investigate the metal−support and to maximize the metal−support interface. By using nanochemistry techniques, we show *for the first time* that Pt or PtAu metal can be created inside each CeO_2 particle with tailored dimensions. The encapsulated metal is shown to interact with the CeO_2 overlayer in an optimum geometry to create a unique interface, giving high activity and excellent selectivity for the water−gas shift (WGS) reaction, but is totally inert for methanation.

Platinum encapsulated in ceria catalysts were synthesized by our modified microemulsion (ME) technique, which had previously been shown to give good control of metal core size and silica coating thickness in silica-encapsulated NM catalysts.[9] In the present case, a cationic surfactant, cetyltrimethylammonium bromide (CTAB), was added to dry toluene, and a solution of $(NH_4)_2[PtCl_6]$ and $Ce(NO_3)_3$ was added dropwise to toluene to create a microemulsion. An aqueous solution of NaOH was added to the mixture, which was then aged for 6 days. It is known that Ce^{3+} will be oxidized to form Ce^{4+} hydroxyl species in the presence of cationic surfactants under alkaline environments and O_2.[10] This oxidation is coupled with reduction of Pt^{4+} to Pt^0, driving the precipitation inside the micelle. A similar redox co-precipitation of Ce^{3+} and Pt^{4+} in NaOH solution was previously reported such that Pt^0 can be obtained without H_2 pre-reduction.[7] The fundamental difference in our ME process is that the aging process (for polymerization/condensation of cerium hydroxyl species to form ceria) is found to be essential to lead to controlled particle dimensions and total metal encapsulation in ceria inside the micelle. As can be seen from Table 1, the 5% Pt/ceria catalyst prepared by ME shows a low CO chemisorption value (3.0%), even though the sample was pre-reduced in H_2 at 300 °C. Assuming the Pt particles are spherical in shape, this would correspond to a calculated Pt average diameter of 30.4 nm (non-genuine data). However, XRD shows an extremely broad Pt⟨111⟩ peak. According to the Scherrer equation, the average metal crystallite size is actually ≤2 nm. The large discrepancy in metal particle size between the two results can be accounted for only if most metal is encapsulated in ceria such that limited metal surface is exposed. Figure 1 (TEM micrograph) shows the spherical, highly crystalline ceria particles after calcination, showing (111) lattice fringes of 3.12 Å, with each particle 4 ± 1 nm in size and a minor degree of particle aggregation. This diameter agrees well with our previous work with Pt/silica particles prepared with the same *W* (water-to-surfactant) ratio of 30 (which defines the size of the water droplet).[11] Examination of the TEM micrograph at high resolution with contrast optimization clearly reveals the core enriched with Pt (EDX and mapping) inside each ceria particle (with the Pt content depending on the metal precursor content added, see Table 2). This TEM image is structurally somewhat similar to those of Pt/ceria in the SMSI state, where the metal particle is decorated by a few angstroms thick ceria (prepared above 500 °C under reducing conditions; the SMSI is a reversible phenomenon which is different from our encapsulation process whereby the ceria directly deposits onto the Pt rather than this occurring as a result of a subsequent reduction step).[1,2]

The methanation activity of the catalysts was assessed (Table 1), which showed a lower CH_4 production at 400 °C in contrast to conventionally prepared co-precipitated Pt/CeO_2. The inactivity of these materials for methanation is not surprising since ceria coverage can substantially reduce the metal exposure. However, it is interesting that the encapsulated catalysts show comparable WGS activity when compared to Cu/ZnO and Pt/CeO_2 catalysts but with no methane formation, suggesting that the nature of active sites for methanation may not be the same as for WGS or that some metal sites may have been blocked by the ceria.

Further improvement in the encapsulation was achieved when NaOH was added to the metal precursor microemulsion, giving a precipitation within the micelle, followed by *subsequent* addition of cerium(III) nitrate (denoted hereafter as MEs samples). All the MEs samples, prepared in this manner, give CO chemisorption values <2.0%; for example, the MEs 5% Pt/ceria gives metal dispersion <0.8%, and that for MEs 5% Pt/5% Au/ceria is <1.8%. Thus, this bottom-up approach, by first building up the NM core, followed by adding ceria material inside the micelle in a sequential manner, was then used.

An important question arises: can one control/optimize activity and selectivity by engineering the structure/geometry of this new catalyst? Table 2 shows that pure ceria synthesized by the MEs technique gives a crystallite size of 3.7 nm. Note that increasing

† University of Reading.
‡ Johnson Matthey Technology Centre.

10.1021/ja056102c CCC: $30.25

Table 1. Comparison of Methanation and WGS Activities

catalyst	methanation activity[c]	WGS activity[d]	CH_4 prod[e]	disper[f]/ d[g]
$Cu/ZnO/Al_2O_3$[a]	nd	55.4	0.03	nd
co-precipitated 2% Pt/ceria[a]	14.4	58.6	13.6	14.2 (6.4)
impregnated 5% Pt/ceria[a]	12.5	53.2	1.51	20.3 (4.4)
ME 5% Pt/ceria[b]	1.9	49.2	0	3.0 (30.4)
MEs 5% Pt/ceria[b]	nd	62.5	0	0.78 (58.4)
MEs 5% Pt/5% Au/ceria[b,h]	<0.1	70.6	0	1.8 (50.4)

[a] Traditional catalyst. [b] ME prepared Pt in ceria. [c] Methanation expressed as % CO to CH_4 using 8% CO and 32.49% H_2 balanced with N_2 at a GHSV of 84 000 h^{-1} at 400 °C. [d] WGS activity expressed as % CO conversion using 0.77% CH_4, 6.15% CO, 7.68% CO_2, 24.99% H_2, and 23.08% H_2O balanced with N_2 at a GHSV of 108 000 h^{-1} at 400 °C. [e] Methane production (%) during WGS reaction with respect to the input of 0.77% CH_4 (in re-formate) at 500 °C. [f] Metal dispersion (%) by CO chemisorptions. [g] *d* is the theoretical metal diameter based on CO chemisorptions. [h] No WGS activity of MEs 1%Au/ceria.

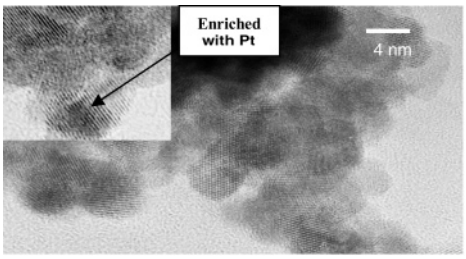

Figure 1. Transmission electron micrograph showing ~4 nm spherical ceria particles (3.12 Å lattice fringes corresponding to CeO_2 (111) are clearly visible) in the ME 5% Pt/ceria (inset shows the enlarged image of an isolated nanoparticle with Pt enrichment in core area).

Table 2. Correlation of Ceria Thickness, Band Transition, and Catalytic Activity

catalyst	ceria thickness (error of ± 0.5 nm)	band transition /eV[b]	WGS/ %
ceria	3.7	3.18	
MEs 1% Pt/ceria	3.6	3.29	0.4
MEs 2.8% Pt/ceria	3.0	3.29	6.6
MEs 5% Pt/ceria[a]	1.7	3.33	62.5
MEs 10% Pt/ceria	4.4	3.31	47.7
MEs 27% Pt/ceria	6.3	3.20	7.6
MEs 5% Pt/5% Au/ceria		3.42	70.6

[a] Metal dispersion (0.78%). [b] See Supporting Information for the band transition evaluation.

the Pt loading from 1 to 5% without altering the cerium content by the MEs technique gives progressively smaller ceria crystallites (ceria size can be accurately derived from XRD line broadening). This is attributed to the increasing size of the inner metal precursor core at increasing metal precursor content, thereby limiting the size of the ceria particle grown in the micelle. It is noted that 5% Pt incorporation is enough to substantially decrease the thickness from 4 (whole sphere) to 1.7 nm (about half a sphere). From diffuse UV reflectance, a blue shift of the absorption edge ($O_{2p}-Ce_{4f}$) of the *n*-type semiconductive ceria upon increasing Pt doping is also observed. A volcano relationship between this band shift and WGS activity is found. These data suggest that an electron-transfer process may take place at the interface between ceria and the metal (with a higher work function) *in facilitating the redox properties of the ceria*.[6,8] The higher blue shift in band transition results in a higher WGS activity. As noted from Tables 1 and 2, MEs PtAu gives the best WGS activity after screening a number of Pt bimetallics, which matches with the highest degree of blue shift. There appears to be a limit on how thin a ceria overlayer can be made over the metal core using the microemulsion method. When metal contents ≥10% are attempted, much larger ceria crystallites are obtained (Table 2). It is known that a water droplet of defined size is stabilized by surfactant assemblies as a soft coating (organized as a micelle). Increasing the size of the metal precursor core could force the cerium hydroxyl species toward the aligned surfactant molecules, leading to destabilization of the system and thus to aggregation and phase segregation. This could account for the blue shift following a volcano shape of dependency on Pt loading as well the activity. But one should not over-interpret the volcano relationship, since it is not yet known whether the overall band shift of the metal-promoted ceria has a progressive linear or complex relationship with the ceria structure at different ceria thicknesses.

It is noted that there is a renewed interest in the WGS for hydrogen production obtained through hydrocarbon re-forming using the NM/ceria. Much current work has been focused for its low-temperature mobile applications (i.e., for fuel cell vehicles) because of it has higher activity than commercial shift catalysts.[3−5] However, for stationary applications, high levels of hydrogen and carbon oxides at elevated pressures and temperatures favor some undesirable side reactions, such as methanation and higher hydrocarbon formation, to take place during the WGS catalysis. Thus, NM/ceria has not been considered for shift catalyst formulation due to its intrinsic poor selectivity for the WGS reaction over the competing reactions of methanation, as these lower the H_2 content of the final feed. Our new NM/ceria nanocatalysts may open up applications in the WGS area.

To conclude, the unusual metal−metal oxide core−shell geometry in this new class of ME catalysts, prepared by nanochemistry techniques, is clearly shown to display some superior catalytic properties over current catalyst systems for WGS.[11] Thus, the ability to assemble functional catalyst particles by a "bottom-up" approach through nanochemistry synthesis, as presently demonstrated, enables catalyst site differentiation for desirable reaction from side reactions within a single catalyst particle.

Supporting Information Available: Detailed sample preparations and material characterizations. This material is available free of charge via the Internet at http://pubs.acs.org.

References

(1) Tauster, S. J.; Fung, S. C.; Garten, R. L. *J. Am. Chem. Soc.* **1978**, *100*, 170.
(2) Bernal, S.; Kaspar, J.; Trovarelli, A. *Catal. Today* **1999**, *50*, 173.
(3) Fu, Q.; Saltsburg, H.; Flytzani-Stephanopoulos, M. *Science* **2003**, *301*, 935.
(4) Tibiletti, D.; Goguet, A.; Meunier, F. C.; Breen, J. P.; Burch, R. *Chem. Commun.* **2004**, 1636.
(5) Ghenciu, A. F. *Curr. Opin. Solid State Mater. Sci.* **2002**, *6*, 389.
(6) Hardacre, C.; Ormerod, R. M.; Lambert, R. M. *J. Phys. Chem.* **1994**, *98*, 10901.
(7) Golunski, S.; Rajaram, R.; Hodge, N.; Hutchings, G. J.; Kiely, C. J. *Catal. Today* **2002**, *72*, 107.
(8) Rajaram, R. R.; Hayes, J. W.; Ansell, G. P.; Hatcher, H. A. U.S. patent 5,993,762, filed on 30 Nov 1999.
(9) Golunski, S.; Rajaram, R. *CATTECH* **2002**, *6*, 30.
(10) Yu, K. M. K.; Yeung, C. M. Y.; Thompsett, D.; Tsang, S. C. *J. Phys. Chem. B* **2003**, *107*, 4515.
(11) Terribile, D.; Trovarelli, A.; Llorca, J.; Leitenburg, C.; Dolcetti, G. *J. Catal.* **1998**, *178*, 299.
(12) Tsang, S. C.; Yeung, C. M. Y.; Thompsett, D. GB patent 0402104.4, filed on 6 Feb 2004.

JA056102C